ISSN 1087-6596, Glass Physics and Chemistry, 2007, Vol. 33, No. 2, pp. 169–173. © Pleiades Publishing, Ltd., 2007.
Original Russian Text © A.V. Osipov, L.P. Mezentseva, I.A. Drozdova, S.K. Kuchaeva, V.L. Ugolkov, V.V. Gusarov, 2007, published in Fizika i Khimiya Stekla.

Crystallization and Thermal Transformations in Nanocrystals of the YPO_4–$LuPO_4$–H_2O System

A. V. Osipov, L. P. Mezentseva, I. A. Drozdova, S. K. Kuchaeva, V. L. Ugolkov, and V. V. Gusarov

Grebenshchikov Institute of Silicate Chemistry, Russian Academy of Sciences, nab. Makarova 2, St. Petersburg, 199034 Russia

e-mail: la_mez@isc.nw.ru

Received September 8, 2006

Abstract—Nanocrystals of yttrium lutetium phosphates of the general formula $Y_{1-x}Lu_xPO_4 \cdot nH_2O$ are synthesized. The temperature dependence of the nanocrystal size is investigated in the range 200–1100°C. The formation of a series of continuous solid solutions belonging to the tetragonal crystal system is revealed, and the limits of their thermal stability are determined.

DOI: 10.1134/S1087659607020125

INTRODUCTION

Considerable recent progress in modern engineering has been made to a large extent owing to the development of new materials and their introduction into full-scale production. Among the new materials, which have appeared, the phosphate-based compounds occupy a highly important place, primarily because they have found a wide use in fabricating protective coating, cements, high-temperature ion-exchangers, laser media, phosphors, etc. [1–3]. Moreover, ceramics based on rare-earth phosphates are considered promising materials for immobilization of radioactive wastes [4]. Preparation of the above materials involves a number of problems that can be solved by changing over to novel technologies based on utilizing nanopowders.

Nanocrystals have often been synthesized using various modifications of the sol–gel method. Analysis of the data presented in [1–3, 5] has demonstrated that hydrated orthophosphates of rare-earth elements (REE) and their solid solutions are formed at a stoichiometric ratio of interacting components (Ln_2O_3 and $NH_4H_2PO_4$ or H_3PO_4) in an aqueous solution in the form of stable colloids that coagulate at pH ≈ 7.

Rare-earth orthophosphates $LnPO_4$ can be divided into two structural subgroups. The first subgroup involves compounds of elements from La to Dy, which crystallize in the hexagonal crystal system upon precipitation from aqueous solutions and contain from 0.5 to 3.0 H_2O molecules per formula unit. These compounds are analogs of the natural mineral rhabdophanite. Upon heating, they lose water and transform into the monoclinic form of the monazite-type mineral [1–3, 5, 6]. Orthophosphates of rare-earth elements from Ho to Lu, as well as Y and Sc, usually crystallize in the tetragonal structure of the natural mineral xenotime and, after precipitation, contain approximately two water molecules [1–3, 5].

The dehydration of REE orthophosphates (REE = Ho–Lu, Y, Sc) proceeds in the temperature range 150–450°C with the complete removal of water. According to the data presented in [1–3, 5, 6], the dehydration does not bring about structural transformations; i.e., the compounds retain the xenotime structure. The data reported in [1–4] indicate that the tetragonal structure is formed by chains consisting of lanthanide polyhedra LnO_8 alternating with phosphate groups PO_4. In each chain, the coordination polyhedra of rare-earth ions are joined together through edges of the PO_4 tetrahedra and the chains themselves are arranged along the *a*–*c* diagonal. Each of these chains is transversely linked to four adjacent REE–O bonds, which are strictly perpendicular to the direction of the chains.

Mezentseva et al. [7, 8] described the phase diagrams of Ln_2O_3–P_2O_5 binary systems and determined the mutual solubility of components in the $LaPO_4$–$NdPO_4$ and $LaPO_4$–$YbPO_4$ systems.

In [9–11], it was demonstrated that, as the size of crystals decreases to nanometers, their structure can undergo a transformation and the ability of components to mutual solubility can change. In this respect, it was of interest to investigate the influence of the particle size on the structure and phase transformations of crystals and on the mutual solubility of the initial components.

In this work, we investigated the formation of nanocrystals in the YPO_4–$LuPO_4$–H_2O system, in which mixed crystals are formed from yttrium and lutetium orthophosphates. Both orthophosphates belong to the same structural type (space group *I*41/*amd*); however, they have different unit cell parameters

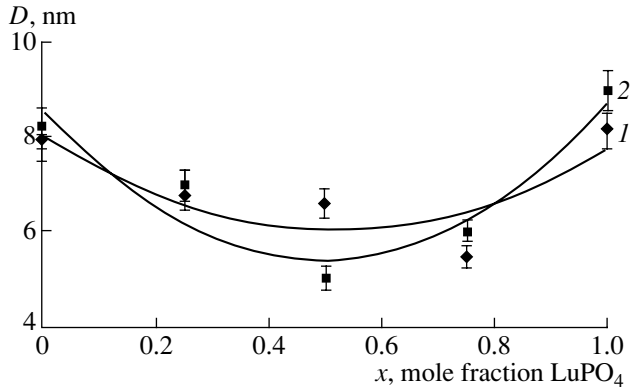

Fig. 1. Dependences of the nanoparticle size on the lutetium concentration x in the $Y_{1-x}Lu_xPO_4 \cdot nH_2O$ samples according to (*1*) X-ray powder diffraction and (*2*) electron microscopy.

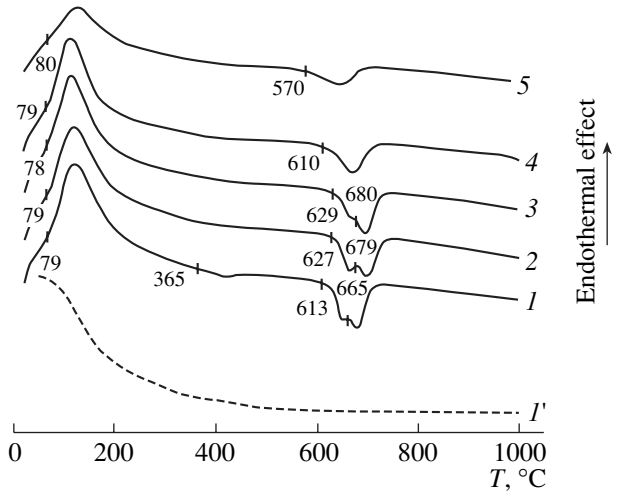

Fig. 2. DSC curves for the $Y_{1-x}Lu_xPO_4 \cdot nH_2O$ samples at lutetium concentrations x = (*1*) 0.0, (*2*) 0.25, (*3*) 0.50, (*4*) 0.75, and (*5*) 1.00. (*1'*) TG curve for the $YPO_4 \cdot nH_2O$ sample.

(YPO_4: a = 6.885 Å, c = 5.982 Å, V = 143.37 Å^3 [12]; $LuPO_4$: a = 6.7938 Å, c = 5.9582 Å, V = 137.5 Å^3 [13]).

SAMPLE PREPARATION AND EXPERIMENTAL TECHNIQUE

Yttrium and lutetium orthophosphates and mixed crystals based on these compounds were prepared from the following initial materials: Y_2O_3 (ItO–Lyum OST 48-4-191-72), Lu_2O_3 (LyuO-D OST 48-207-81), monosubstituted ammonium phosphate (special-purity grade), nitric acid (special-purity grade), aqua ammonia (special-purity grade), and distilled water.

Phosphate samples were synthesized through precipitation with $NH_4H_2PO_4$ at room temperature and pH ≈ 7 from solutions of yttrium and lutetium nitrates prepared by the dissolution of the corresponding oxides in nitric acid. The precipitates were kept in the mother liquor for 24 h, washed by decantation, filtered off, and dried at a temperature of 110°C in air.

X-ray powder diffraction analysis was performed using X-ray powder diffraction patterns recorded on a Siemens D-500HS X-ray diffractometer (Germany) and a DRON-3 diffractometer (CuK_α radiation).

The nanoparticle size was determined from the broadening of the diffraction peaks according to the Scherrer formula and with the use of transmission electron microscopy on an EM-125 electron microscope (U_{acc} = 75 kV).

The thermal behavior of the samples was examined by differential scanning calorimetry (DSC) and thermal gravimetry (TG). The investigations were carried out on an STA 429 (NETZSCH) calorimeter. The onset of the thermal effect was determined from the intersection of the tangents to the base line of the DSC curve and to the branch of the thermal peak.

The kinetics of nanocrystal growth was investigated under annealing–quenching conditions with the subsequent determination of the particle size by the above methods. Heat treatment of pelleted samples was performed in air at temperatures in the range 200–1100°C with isothermal holding for 1 h.

RESULTS AND DISCUSSION

Orthophosphates of the general formula $Y_{1-x}Lu_xPO_4 \cdot nH_2O$ (x = 0.0, 0.25, 0.50, 0.75, 1.00) were synthesized by the technique described above. The data obtained from X-ray powder diffraction (Fig. 1, curve *1*) and transmission electron microscopy (Fig. 1, curve *2*) indicate that the sizes of $Y_{1-x}Lu_xPO_4 \cdot nH_2O$ orthophosphate particles are of nanometer scale. Moreover, according to electron microscopy, the samples under investigation contain both nanoparticles in the form of thin plates that are isometric in the developed plane and a great amount of sufficiently large agglomerates of nanoparticles.

Figure 2 presents the data obtained by the DSC and TG methods. The DSC curve of the $YPO_4 \cdot nH_2O$ sample is characterized by four thermal effects. The onset of the first (endothermal) effect is observed at a temperature of 79°C, whereas the following three (exothermal) effects begin to manifest themselves at temperatures of 365, 613, and 665°C, respectively. The endothermal effect is accompanied by a considerable weight loss of the sample (Fig. 2, curve *1'*). Note that the character of the first thermal effect remains virtually unchanged as the concentration of Lu^{3+} ions in mixed crystals increases (Fig. 2). The onset of the exothermal effects shifts as the lutetium concentration increases. It

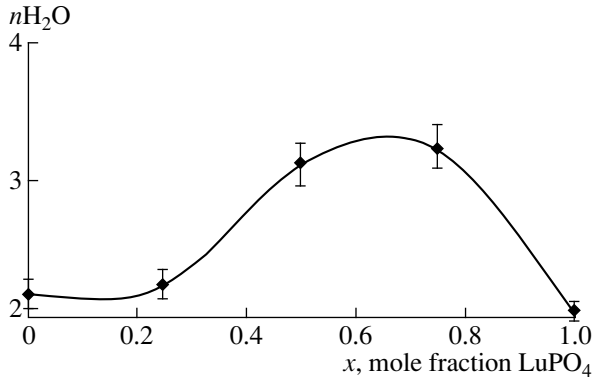

Fig. 3. Dependence of the number of water molecules n in the $Y_{1-x}Lu_xPO_4 \cdot nH_2O$ nanocrystals on the lutetium concentration x.

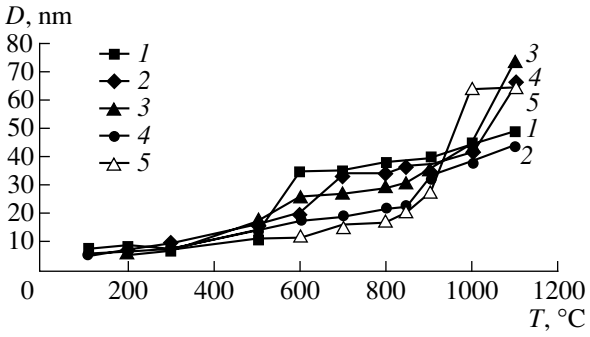

Fig. 4. Dependences of the particle size D on the annealing temperature (τ = 1 h) for the $Y_{1-x}Lu_xPO_4 \cdot nH_2O$ samples at lutetium concentrations x = (*1*) 0.0, (*2*) 0.25, (*3*) 0.50, (*4*) 0.75, and (*5*) 1.00.

is worth noting that two of the three exothermal peaks, which are observed at higher temperatures, merge into a more extended peak with the onset at 610°C for the sample of the composition $Y_{0.75}Lu_{0.25}PO_4 \cdot nH_2O$ and at 570°C for $LuPO_4$.

The number of water molecules per formula unit of the orthophosphate was determined from the data on the weight loss of the samples (Fig. 3). It follows from the results obtained that the highest water content corresponds to the $Y_{1-x}Lu_xPO_4 \cdot nH_2O$ nanocrystals at x = 0.5–0.8. This correlates with their sizes (Fig. 1), which are smaller as compared to nanocrystals of the other compositions, and, consequently, with the larger specific surface and, therefore, with the higher adsorption capacity.

Figure 4 shows the dependences of the particle size D on the temperature of annealing for 1 h. A comparison of the data presented in Figs. 2 and 4 allows us to conclude that the exothermal peaks in the DSC curves are associated with the crystallization of precipitated products. This process is accompanied by an increase in the nanocrystal sizes in the temperature range corresponding to the exothermal effects. The weak exothermal effects observed in the temperature range 365–445°C, can also be attributed to the change in the morphology of crystals from thin nanoplates, which are formed upon the nucleation and growth of nanoparticles, to rounded grains in pelleted samples [14].

The X-ray powder diffraction patterns shown in Figs. 5 and 6 indicate the existence of a continuous series of solid solutions between the yttrium and lutetium orthophosphates over the entire temperature range 200–1100°C. These solid solutions belong to the tetragonal crystal system.

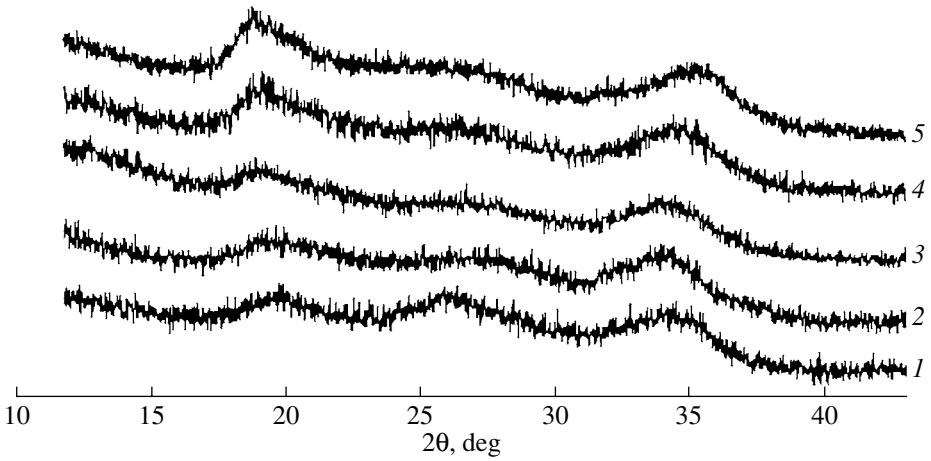

Fig. 5. X-ray powder diffraction patterns of the $Y_{1-x}Lu_xPO_4 \cdot nH_2O$ precipitates at lutetium concentrations x = (*1*) 0.0, (*2*) 0.25, (*3*) 0.50, (*4*) 0.75, and (*5*) 1.00.

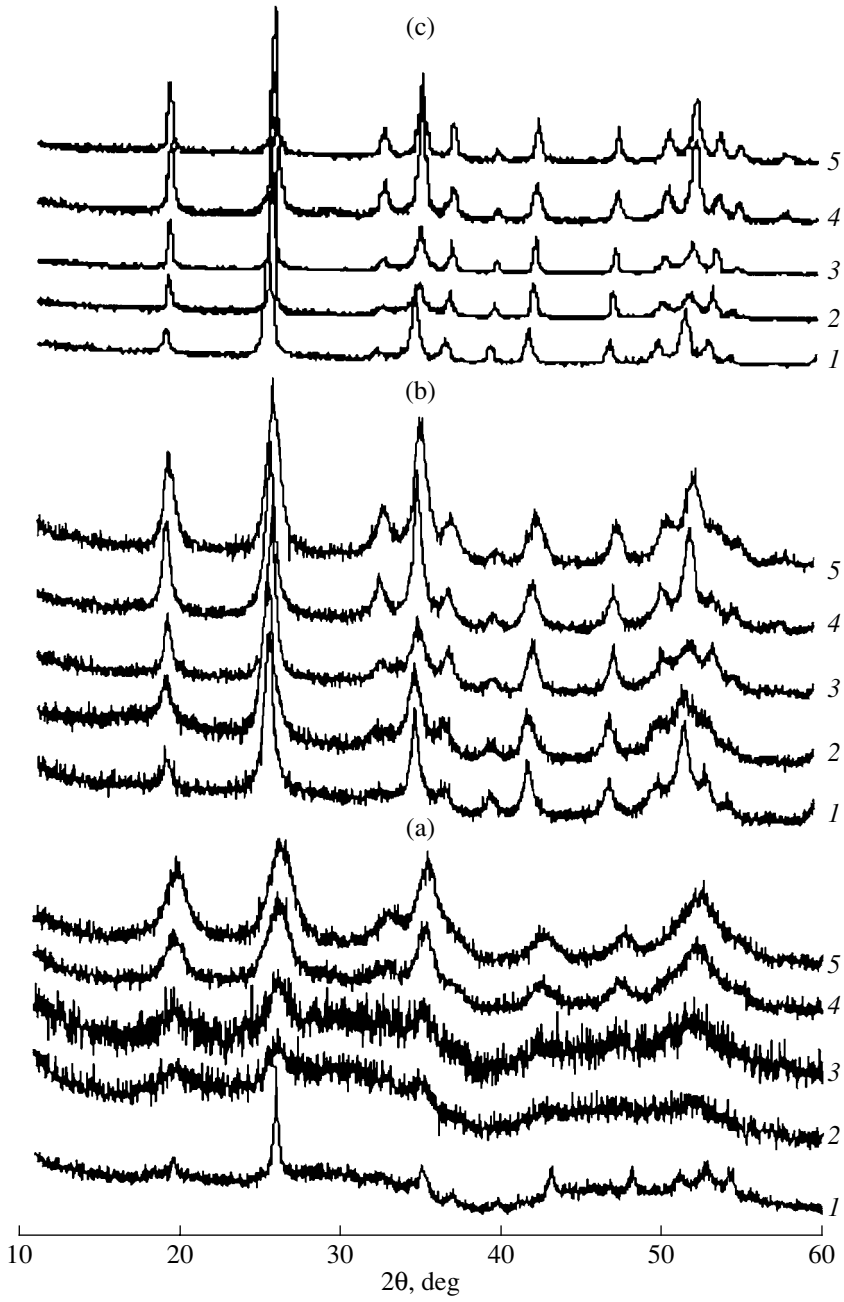

Fig. 6. X-ray powder diffraction patterns of the $Y_{1-x}Lu_xPO_4 \cdot nH_2O$ samples at lutetium concentrations x = (*1*) 0.0, (*2*) 0.25, (*3*) 0.50, (*4*) 0.75, and (*5*) 1.00 after annealing at temperatures of (a) 500, (b) 850, and (c) 1100°C.

The analysis of the dependences of the nanocrystal size on the annealing temperature (Fig. 4) revealed two characteristic temperatures, namely, T_1 = 500°C and T_2 = 900°C, at which the growth rate of nanoparticles increases abruptly. This phenomenon is most likely explained by the activation of mass transfer over the surface and throughout the bulk of nanoparticles at these temperatures. The data obtained indicate that these temperatures depend weakly on the concentrations of components in the series $Y_{1-x}Lu_xPO_4$.

CONCLUSIONS

Thus, nanocrystals of yttrium lutetium phosphates of the general formula $Y_{1-x}Lu_xPO_4 \cdot nH_2O$ (x = 0.0, 0.25, 0.50, 0.75, 1.00) were synthesized. It was established that, in the temperature range 200–1100°C, yttrium lutetium orthophosphates form a continuous series of solid solutions belonging to the tetragonal crystal system. The structural state of the solid solutions was found to be independent of the particle size, at least, in the range from 6–8 to 40–80 nm. It was

revealed that there are two characteristic temperatures, namely, 500 and 900°C, at which the nanocrystal size increases abruptly.

ACKNOWLEDGMENTS

This study was supported by the Russian Foundation for Basic Research, project no. 06-03-32780-a.

REFERENCES

1. Bondar', I.A., Vinogradova, N.V., Dem'yanets, L.N., *et al.*, *Soedineniya redkozemel'nykh elementov: Silikaty, germanaty, fosfaty, arsenaty, vanadaty* (Rare-Earth Element Compounds: Silicates, Germanates, Phosphates, Arsenates, and Vanadates), Moscow: Nauka, 1983 [in Russian].
2. Litvin, B.N. and Masloboev, V.A., *Redkozemel'nye fosfaty* (Rare-Earth Phosphates), Leningrad: Nauka, 1989 [in Russian].
3. Portnoi, K.I. and Timofeeva, N.I., *Kislorodnye soedineniya redkozemel'nykh elementov. Spravochnik* (A Handbook on Oxygen-Containing Compounds of Rare-Earth Elements), Moscow: Metallurgiya, 1986 [in Russian].
4. Ushakov, S.V., Helean, K.B., Navrotsky, A., and Boather, L.A., Thermochemistry of Rare-Earth Orthophosphates, *J. Mater. Res.*, 2001, vol. 16, no. 9, pp. 2623–2633.
5. Bondar', I.A., Domanskii, A.I., Mezentseva, L.P., Degen, M.G., and Kalinina, N.E., Physicochemical Investigations of Rare-Earth Orthophosphates, *Zh. Neorg. Khim.*, 1976, vol. 21, no. 8, pp. 2045–2050.
6. Yaglov, V.N., Chemistry and Thermodynamics of Orthophosphate Hydrates, *Extended Abstract of Doctoral Dissertation*, Minsk: Belarussian Technological Institute, 1980 [in Russian].
7. Mezentseva, L.P., Phase Diagrams of the Ln_2O_3–P_2O_5 Binary Systems and Solid Solutions of Rare-Earth Element Phosphates, *Extended Abstract of Candidate's Dissertation*, Leningrad: Institute of Silicate Chemistry, 1983 [in Russian].
8. Mezentseva, L.P., Kosulina, G.I., Grebenshchikov, R.G., and Udalov, Yu.P., *Diagrammy sostoyaniya sistem tugoplavkikh oksidov. Spravochnik. Vyp. 5. Dvoinye sistemy. Chast' 2* (A Handbook on Phase Diagrams of High-Melting Oxide Systems: Binary Systems), Galakhov, F.Ya, Ed., Leningrad: Nauka, 1986, issue 5, part 2 [in Russian].
9. Gusarov, V.V., Statics and Dynamics of Polycrystalline Systems Based on High-Melting Oxides, *Extended Abstract of Doctoral Dissertation*, St. Petersburg: St. Petersburg State Technological Institute (Technical University), 1996 [in Russian].
10. Pozhidaeva, O.V., Korytkova, E.N., Romanov, D.P., and Gusarov, V.V., Formation of Zirconium Dioxide Nanocrystals in Hydrothermal Media of Different Chemical Compositions, *Zh. Obshch. Khim.*, 2002, vol. 72, no. 6, pp. 910–914 [*Russ. J. Gen. Chem.* (Engl. transl.), 2002, vol. 72, no. 6, pp. 849–853].
11. Ul'yanova, T.M., Zub, E.M., and Krut'ko, N.P., X-ray Diffraction Investigations of the Phase Transitions and Interaction of Components in the ZrO_2–Al_2O_3 System, *Poverkhnost,* 2002, no. 7, pp. 49–53.
12. *JCPDS 5-454.*
13. *JCPDS 43-3.*
14. Bondar', I.A., Degen, M.G., Mezentseva, L.P., and Koroleva, L.N., Formation and Growth Processes of Rare-Earth Niobates and Phosphates, *Ceramurgia Int.*, 1980, vol. 6, no. 7, pp. 148–150.